In vivo biotinylation of the vasculature in B-cell lymphoma identifies BST-2 as a target for antibody-based therapy

*Christoph Schliemann,[1] *Christoph Roesli,[1] Haruhiko Kamada,[1,2] Beatrice Borgia,[1] Tim Fugmann,[1] Wolfram Klapper,[3] and Dario Neri[1]

[1]Institute of Pharmaceutical Sciences, Department of Chemistry and Applied Biosciences, ETH Zurich, Zurich, Switzerland; [2]Laboratory of Pharmaceutical Proteomics, National Institute of Biomedical Innovation, Osaka, Japan; and [3]Institute of Pathology, Section Hematopathology and Lymph Node Registry, University Hospital Schleswig-Holstein, Kiel, Germany

The discovery of accessible markers of lymphoma may facilitate the development of antibody-based therapeutic strategies. Here, we describe the results of a chemical proteomic study, based on the in vivo biotinylation of vascular proteins in lymphoma-bearing mice followed by mass spectrometric and bioinformatic analysis, to discover proteins expressed at the tissue-blood border of disseminated B-cell lymphoma. From a list of 58 proteins, which were more than 10-fold up-regulated in nodal and extranodal lymphoma lesions compared with their levels in the corresponding normal host organs, we validated BST-2 as a novel vascular marker of B-cell lymphoma, using immunochemical techniques and in vivo biodistribution studies. Furthermore, targeting BST-2 with 2 independent monoclonal antibodies delayed lymphoma growth in a syngeneic mouse model of the disease. The results of this study delineate a strategy for the treatment of systemic B-cell lymphoma in humans and suggest that anti–BST-2 antibodies may facilitate pharmacodelivery approaches that target the tumor-stroma interface. (Blood. 2010;115: 736-744)

Introduction

Monoclonal antibodies are increasingly being used in modern anticancer therapy either as intact immunoglobulins or as carriers for the selective delivery of bioactive molecules (eg, drugs with cleavable linkers, radionuclides, cytokines) to the tumor site, thereby minimizing exposure to noninvolved organs.[1-6] Initially, site-directed cancer therapies have mainly aimed at targeting antigens expressed on the surface of cancer cells. However, tumor cells embedded in large tumor masses are not readily accessible to antibodies from the bloodstream,[7] an obstacle that may reduce their in vivo therapeutic efficacy despite a sufficient activity in vitro. Recently, pharmacodelivery strategies have been developed that target molecules expressed in tumor blood vessels or in the tumor stroma.[1,3,6] Indeed, structures in the immediate vicinity of the tissue-blood border are not only inherently accessible to blood-borne agents but also allow some unique therapeutic options. For example, the angiogenic endothelium appears exceptionally suited for the selective shutdown of a tumor's blood supply.[8] Components of the subendothelial extracellular matrix are often more abundantly expressed, permitting an efficient antibody-mediated deposition of bioactive payloads at the tumor site.[9-14]

Antibody-based pharmacodelivery strategies are particularly attractive for the therapy of hematologic malignancies, in light of the fact that patients with leukemias or lymphomas commonly experience serious side effects from conventional induction chemotherapies. The advent of monoclonal antibodies specific to certain CD antigens represented a significant step toward a more specific therapy of these malignancies, either unconjugated (eg, rituximab or alemtuzumab) or as carriers for cytotoxic drugs (eg, gemtuzumab ozogamicin) or radionuclides (eg, ibritumomab tiuxetan).[15] Whereas cell-surface antigens have been extensively characterized and exploited for antibody-based targeted therapies over the years,[15,16] lymphoma-specific markers expressed in the vascular[13,14] or stromal[17] compartment have attracted less attention so far. Very recently, the extra domain B (EDB) of oncofetal fibronectin, a marker of angiogenesis, has been proposed as an antigen for vascular-targeted pharmacodelivery strategies in lymphoma, based on immunohistochemical findings and on preclinical and clinical studies with the EDB-targeted immunocytokine L19-IL2 and the radiolabeled antibody ^{131}I-L19.[13,14] Indeed, this radiopharmaceutical could eradicate aggressive lymphomas in patients who had previously failed to respond to multiple lines of chemotherapy and radiotherapy. L19-IL2 was found to potently synergize with the anti-CD20 antibody rituximab, eradicating localized and systemic B-cell lymphomas in mice that could not be cured with either agent alone.[13] These promising results provide a strong motivation to continue the search for vascular markers of lymphoma that may be drugged with antibodies.

Our group has developed a general chemical proteomics approach for the identification of proteins that are readily accessible from the bloodstream. The method relies on the covalent labeling of vascular proteins by in vivo perfusion of tumor-bearing animals[18,19] or by ex vivo perfusion of surgically resected human organs,[20] using reactive ester derivatives of biotin. The resulting biotinylated proteins can be efficiently recovered from normal and pathologic tissues by purification on

Submitted August 17, 2009; accepted October 15, 2009. Prepublished online as *Blood* First Edition paper, November 10, 2009; DOI 10.1182/blood-2009-08-239004.

The online version of this article contains a data supplement.

The publication costs of this article were defrayed in part by page charge payment. Therefore, and solely to indicate this fact, this article is hereby marked "advertisement" in accordance with 18 USC section 1734.

*C.S. and C.R. contributed equally to this study and share first authorship.

streptavidin resins.[19] On-resin proteolytic digestion of biotinylated proteins, nano–high-performance liquid chromatography (HPLC) separation of resulting peptides, and their identification and relative quantification in the presence of internal standards by tandem mass spectrometry,[21] allow the characterization of atlases of circulation-accessible proteins in normal organs and at sites of disease, thus facilitating the discovery of novel markers of pathology.

Here, we describe the in vivo biotinylation of immunocompetent mice bearing syngeneic disseminated A20 B-cell lymphoma, using a terminal perfusion procedure. The A20 lymphoma model is known to closely mimic histopathologic aspects and the anatomic distribution of large B-cell lymphoma in humans, recapitulating nodal and extranodal tumor growth in various organs.[22] Comparative proteomic analyses of lymphoma lesions and their corresponding host organs allowed the identification of a repertoire of differentially expressed bloodstream-accessible proteins. One highly promising candidate, BST-2, has been investigated in detail, revealing a restricted expression at lymphoma vascular sites, which could be targeted in vivo using anti–BST-2 antibodies. Furthermore, 2 anti–BST-2 monoclonal antibodies substantially reduced tumor growth in vivo, thus suggesting that this antigen may be suitable for therapeutic strategies both with intact immunoglobulins and with judiciously chosen antibody derivatives.

Methods

Animal model

The A20 murine B-cell lymphoma cell line was purchased from ATCC. Six- to 8-week-old female BALB/c mice were obtained from Charles River Laboratories. Systemic B-cell lymphoma was induced by injection of 2×10^6 A20 cells into the tail vein.[22] Twenty-four to 26 days after injection, 12 mice bearing disseminated A20 lymphoma and 6 age-matched healthy mice were subjected to the in vivo protein biotinylation procedure. All animal experiments were approved by the Swiss Federal Veterinary Office (license 198/2005).

In vivo protein biotinylation

In vivo biotinylation experiments were performed as previously described.[18,19] After perfusion with the reactive ester derivative of biotin, organs and tumors were excised and specimens were either snap-frozen for preparation of organ homogenates or embedded in cryoembedding compound (Thermo Fisher Scientific) and frozen for histochemical analysis.

Preparation of protein extracts

Lymphoma lesions and their corresponding host organs were resuspended in lysis buffer (2% sodium dodecyl sulfate [SDS], 50mM Tris, 10mM ethylenediaminetetraacetic acid, CompleteE proteinase inhibitor cocktail [Roche Diagnostics] in phosphate-buffered saline [PBS], pH 7.4), using 40 μL/mg tissue. The specimens were then homogenized using an Ultra-Turrax T8 disperser (IKA-Werke) and sonicated using a Vibra-cell (Sonics), followed by 15 minutes of incubation at 95°C and 20 minutes' centrifugation at 15 000*g*. The resulting supernatants ("total protein extracts") were used for the subsequent capture step on streptavidin-resin. The protein concentration of the total protein extracts was determined with the BCA Protein Assay Reagent Kit (Thermo Fisher Scientific).

Purification of biotinylated proteins

For each sample, 400 μL of streptavidin-sepharose (GE Healthcare) slurry were washed 3 times with buffer A (1% NP40, 0.1% SDS in PBS), pelleted, and mixed with 5 mg of total protein extract. The capture of biotinylated proteins was allowed to proceed for 2 hours at room temperature in a revolving mixer. The supernatant was removed, and the resin was washed 3 times with buffer A, twice with buffer B (0.1% SDS, 2M NaCl in PBS, 40°C), and 8 times with digestion buffer (50mM Tris-HCl, 1mM $CaCl_2$, pH 8.0). Finally, the resin was resuspended in 200 μL of digestion buffer and 20 μL of sequencing grade modified porcine trypsin (stock solution of 80 ng/μL in digestion buffer; Promega) were added. Tryptic digestion was carried out overnight at 37°C under constant agitation. Peptides were desalted, purified, and concentrated with C_{18} microcolumns (Varian Inc). After lyophilization, peptides were stored at −20°C.

Nanocapillary reverse-phase HPLC with online fraction spotting onto MALDI plates

Tryptic peptides were separated by reverse-phase HPLC using an UltiMate nanoscale LC system and a FAMOS microautosampler (LC Packings) controlled by the Chromeleon software (Dionex). Mobile phase A consisted of 5% acetonitrile and 0.1% trifluoroacetic acid (TFA) in water, mobile phase B of 80% acetonitrile, and 0.1% TFA in water. The flow rate was 300 nL/minute. Lyophilized peptides derived from the digestion of biotinylated protein affinity purified from 2 mg of total protein were dissolved in 5 μL of buffer A and loaded on the column (inner diameter, 75 μm; length, 15 cm; filled with C_{18} PepMap 100, 3-μm, 100-Å beads; LC Packings). The peptides were eluted with a gradient of 0% B for 3 minutes, 0% to 52% B for 82 minutes, 52% to 100% B for 10 minutes, and 100% B for 5 minutes; the column was equilibrated with 100% A for 20 minutes before analyzing the next sample. Eluting fractions were mixed with a solution of 3 mg/mL α-cyano-4-hydroxycinnamic acid, 277pmol/mL of each of the 4 internal standard peptides ([des-arg^9]-bradykinin, neurotensin, angiotensin I, and adrenocorticotropic hormone fragment 1-17; all from Sigma-Aldrich), 0.1% TFA, and 70% acetonitrile in water and deposited on a blank matrix-assisted laser desorption/ionization (MALDI) target plate (416 spots per sample) using an online Probot system (Dionex). The final concentration of each internal standard peptide was 50fmol per spot.

MALDI-TOF/TOF mass spectrometry

MALDI–time-of-flight (TOF)/TOF analysis was carried out with the 4800 MALDI TOF/TOF Analyzer (Applied Biosystems). All spectra were acquired with a solid-state laser (355 nm) at a laser repetition rate of 200 Hz. After measuring all samples in the mass spectrometry (MS) mode, a maximum of 15 precursors per spot were automatically selected for subsequent fragmentation by collision-induced dissociation. Resulting spectra were processed and analyzed using both the ProteinPilot software (Applied Biosystems; Paragon algorithm) and the Global Protein Server Workstation (Applied Biosystems; using internal MASCOT Matrix Science), for matching MS and MS/MS data against databases of in silico digested proteins. The data obtained were screened against a database of all mouse proteins downloaded from the European Bioinformatics Institute homepage (ftp.ebi.ac.uk/pub/databases/SPproteomes/fasta/proteomes/59.M_musculus.fasta.gz). The following settings were used for the identification of peptides and proteins: (1) precursor tolerance, 20 ppm; (2) MS/MS fragment tolerance, 0.25 Da; (3) maximal missed cleavages, one; and (4) variable modification, one (oxidation of methionine). Peptides were considered correct calls when the confidence interval was greater than 95%. To reduce redundancies in protein identification, data were processed further using ProteinCenter software (Proxeon).

Relative protein quantification by DeepQuanTR software

The DeepQuanTR software has been described in detail elsewhere (T.F., D.N., C.R., manuscript submitted). Briefly, after MS acquisition, data related to the individual peaks (fractions, intensities, m/z ratios) were loaded into the DeepQuanTR software, which performed a normalization of individual signal intensities to the internal standard peptides and an annotation (peptide identification and association with a parent protein). Normalized intensities for the individual peptides from all samples were used for the computation of DeepQuanTR peptide and protein scores, indicating the relative abundance of individual peptides and proteins in the various groups of samples.

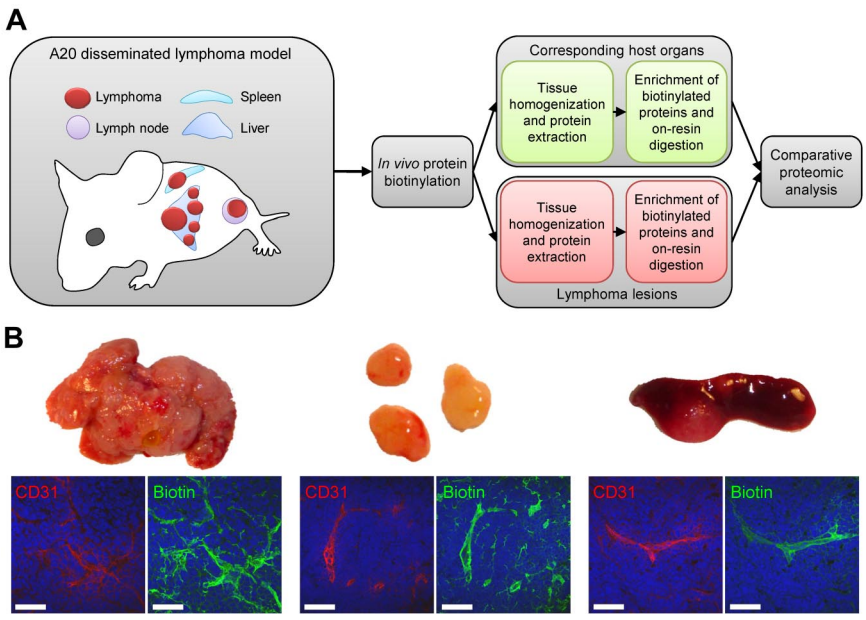

Figure 1. In vivo biotinylation of the bloodstream-accessible tissue compartment in a syngeneic mouse model of B-cell lymphoma. (A) Healthy and lymphoma-bearing mice were subjected to the terminal perfusion with a reactive ester derivative of biotin, leading to the covalent modification of proteins accessible from the bloodstream. Tumors and corresponding normal organs were excised and homogenized for the preparation of total protein extracts. Biotin-tagged proteins were enriched on streptavidin Sepharose, on-resin digested with trypsin, resulting peptides were separated by nanocapillary reverse-phase HPLC, and submitted to the comparative proteomic analysis. (B) Streptavidin-based detection of biotinylated structures (green) in perfused lymphoma tissues harvested from liver, lymph nodes, and spleen, in relation to vascular endothelium (CD31, red). Scale bars represent 50 μm.

Immunofluorescence analysis

Dual-color immunofluorescence was performed on 10-μm acetone-fixed cryostat sections. The following antibodies were used for immunostainings: rat anti–mouse activated leukocyte cell adhesion molecule (CD166), rat anti–mouse CD98, rat anti–mouse BST-2 (129c), and rat anti–mouse BST-2 (927) from eBioscience; rat anti–mouse endoglin, goat anti–mouse EMILIN-1, and rabbit anti–mouse PECAM-1 from Santa Cruz Biotechnology; rat anti–mouse transferrin receptor from Abcam; rat anti–mouse CD205 from AbD Serotec; goat anti–mouse clusterin from R&D Systems; rat anti–mouse PECAM-1 from BD Biosciences; and mouse anti–human BST-2 from Abnova. Appropriate Alexa Fluor 488– or 594–labeled secondary antibodies were purchased from Invitrogen. In vivo biotinylated structures were detected using Alexa Fluor 488–conjugated streptavidin (Invitrogen). Nuclei were counterstained with 4,6-diamidino-2-phenylindole (Invitrogen). All slides were examined on a LSM 510 Meta confocal laser scanning microscope (Carl Zeiss).

Analysis of in vivo targeting

To investigate target accessibility in vivo, BALB/c mice bearing disseminated or subcutaneous A20 lymphoma were intravenously injected with 50 μg of monoclonal rat IgGs (anti–BST-2 clones 927 and 129c and isotype control). Six hours after injection, tissues were excised, frozen in optimal cutting temperature (OCT), and stored at −80°C. In vivo injected monoclonal antibodies and ex vivo applied rabbit anti–mouse CD31 were detected using the secondary antibodies donkey anti–rat Alexa Fluor 488 and goat anti–rabbit Alexa Fluor 594. Sections were analyzed on a LSM 510 Meta confocal laser scanning microscope.

Therapy experiments

BALB/c mice were inoculated subcutaneously with 10^7 A20 cells to induce localized lymphoma tumors in the left flank. Five days after injection, when palpable tumor nodules have developed, mice were grouped (n = 5 per group) to maximize uniformity and injected with 5 mg/kg of the monoclonal anti–BST-2 antibody 927, 5 mg/kg of the monoclonal anti–BST-2 antibody 129c, or 5 mg/kg of an isotype control IgG (all antibodies were of the rat IgG2b isotype). Injections were performed once weekly for a total of 3 injections. Tumor volume was measured using a digital caliper and calculated according to the formula $L \times W^2 \times 0.5$ (L indicates length; and W, width).

Immunohistochemistry

Human lymphoma specimens were retrieved from consultation files of the Institute of Pathology, University Hospital Schleswig-Holstein, Kiel, Germany. Cryosections of 6-μm thickness were fixed in chilled acetone, rehydrated in Tris-buffered saline (50M Tris, 100mM NaCl, pH 7.4), and blocked with 20% fetal calf serum (Invitrogen). Mouse anti–human BST-2 antibody (Abnova) was detected using polyclonal rabbit anti–mouse IgG and the alkaline phosphatase–antialkaline phosphatase complex (Dako Denmark). Fast Red (Sigma-Aldrich) was used as phosphatase substrate, and slides were analyzed on an Axiovert S100 TV microscope (Carl Zeiss).

Statistical analysis

Differences in tumor growth among treatment groups were assessed using the Student *t* test. *P* values less than .05 were considered significant.

Results

In vivo protein biotinylation of disseminated B-cell lymphoma

Twelve lymphoma-bearing mice and 6 age-matched healthy BALB/c mice were subjected to a terminal perfusion procedure for the in vivo biotinylation of accessible proteins (Figure 1A). After anesthesia, the systemic circulation was perfused by intracardiac administration of an aqueous solution of Sulfo-NHS-LC-biotin (1 mg/mL, 10 mL) over 10 minutes at 100 mm Hg, followed by perfusion with quenching solution to block unreacted biotin ester. The efficient biotinylation of proteins in the most accessible structures (vascular endothelial cells, subendothelial extracellular matrix, and perivascular tumor and stroma cells) was confirmed using a streptavidin-based detection method (green fluorescent staining in Figure 1B), as illustrated by CD31 costaining (red) in lymphoma lesions from liver, lymph nodes, and spleen. After in vivo biotinylation, normal organs and lymphoma tissues were excised, homogenized in the presence of 2% SDS, and submitted to chromatography on streptavidin-Sepharose. After extensive washing, biotinylated proteins were tryptically digested on-resin. The resulting peptides were separated by reverse-phase nano-HPLC, mixed with constant amounts of 4 commercially available peptides

serving as internal standards for relative quantification, and analyzed by MALDI-TOF and MALDI-TOF/TOF mass spectrometry.

Bioinformatic processing of MS data

The DeepQuanTR software, which allows a pairwise comparison of the average normalized signal intensities for multiple tryptic peptides corresponding to the same protein in different tissue samples, was used to identify differentially expressed proteins in pairs of lymphoma lesions and their corresponding normal organs (hepatic lymphoma vs normal liver, nodal lymphoma vs normal lymph nodes, splenic lymphoma vs normal spleen). We identified 520 nonredundant proteins with 2 or more peptides in liver, 295 in lymph node, and 368 in spleen samples (supplemental Table 1, available on the *Blood* website; see the Supplemental Materials link at the top of the online article). Color-coded DeepQuanTR-computed expression values of all accessible proteins identified in lymphoma lesions grown in liver, lymph nodes, and spleen can be found as supplemental Figure 1. Proteins up-regulated in individual lymphoma samples compared with the average protein expression in the corresponding healthy host organ were coded in green, and down-regulated proteins were displayed in red. The color intensity relates to the magnitude of the differences in MS signal intensities (supplemental Figure 1).

Virtually all lymphoma-associated cell-surface antigens identified so far are also expressed on their nonmalignant counterparts as well.[15] Thus, we focused our attention on antigens that were consistently up-regulated at all anatomic lymphoma localizations. In this analysis, all proteins identified with 2 or more peptides in at least 1 of the 3 lymphoma localizations were included. A total of 271 proteins were identified in all 3 lymphoma-normal organ pairs; 58 of them were up-regulated more than 10-fold in hepatic, nodal, and splenic lymphoma lesions (corresponding to an average DeepQuanTR value > 2.30). A selection of differentially expressed candidates is presented in Figure 2. These proteins include ITI-HC3, transferrin receptor, fibulin-2, PK-120, leucyl-cystinyl aminopeptidase, bone marrow stromal antigen 2 (BST-2, CD317), activated leukocyte cell-adhesion molecule (CD166), EMILIN-1, basigin, elastin, tubulointerstitial nephritis antigen-like, clusterin, and CD98 heavy chain. Classic endothelial or extracellular matrix proteins previously known to be involved in tumor angiogenesis and/or proposed as targets for vascular targeting applications, such as endoglin (CD105), lactadherin, vitronectin, thrombospondin-1, fibronectin, tenascin-C, MECA-32, PECAM-1 (CD31), aminopeptidase N (CD13), CD36, and several collagens and integrins, were also identified (Figure 2; supplemental Table 1). Literature findings for proteins previously known to be expressed in lymphomas and/or during angiogenesis for a selection of the 58 proteins that were more than 10-fold up-regulated are presented in supplemental Table 2.

Validation of accessible lymphoma targets

To validate the DeepQuanTR findings, we focused our attention on a subset of candidate antigens for which antibodies suitable for immunofluorescence were available. Eight proteins were studied in detail by immunofluorescence analysis of the tumor/normal liver border, which confirmed the protein expression data derived from the DeepQuanTR analysis (Figure 3). Costaining with CD31 revealed a vascular pattern of staining for certain antigens, including novel (eg, BST-2) and previously known (eg, endoglin) markers of angiogenesis, as well as matrix components (eg, clusterin) or proteins expressed on the surface of tumor cells (eg, transferrin receptor, or CD98). Higher magnification confocal images of all candidate proteins in relation to CD31 staining are presented in supplemental Figure 2. Some of the proteins identified

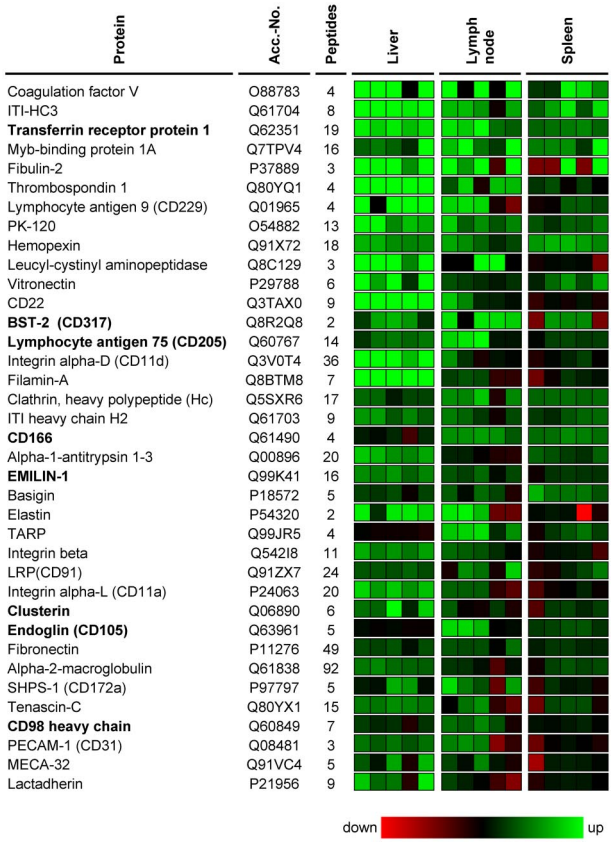

Figure 2. Selection of proteins overexpressed at all 3 lymphoma localizations. A selection of proteins that were consistently found up-regulated at nodal and extranodal lymphoma localizations is shown. Protein abundances in 5 lymphoma samples are displayed for each organ/lymphoma pair with a color code related to the corresponding DeepQuanTR score (maximum = e^6-fold up-regulation; minimum = e^6-fold down-regulation). Proteins up-regulated in comparison to the average protein expression in the corresponding normal host organ are displayed in green, down-regulated proteins in red. Proteins are sorted in descending order according to the average regulation score calculated from all 3 localizations. Antigens selected for further investigation are marked in bold.

appeared to be completely undetectable in adjacent normal liver tissue with a clear-cut margin of staining at the normal tissue/lymphoma border (eg, BST-2, clusterin, or EMILIN-1). Others displayed a considerable expression also in normal tissue, yet at a lower intensity compared with their expression in lymphoma lesions (eg, endoglin, CD98; Figure 3).

BST-2 as a novel marker of lymphoma blood vessels

BST-2 was one of the most interesting vascular markers of lymphoma identified in the chemical proteomic analysis. To the best of our knowledge, a vascular expression of the BST-2 protein in tumors had not been described before. In light of the excellent colocalization of BST-2 with the vascular marker CD31 in lymphoma blood vessels, while the antigen was completely undetectable in normal liver, we decided to further explore BST-2 as a potential lymphoma vascular target for antibody-based pharmacodelivery applications and therapy. First, we performed systematic immunofluorescence expression studies of normal mouse organs (Figure 4A). BST-2 (green) was virtually undetectable in the vasculature of all organs analyzed, including brain, heart, lung, liver, spleen, lymph nodes, kidney, intestine, kidney, and skeletal muscle, whereas CD31 (red) was always detectable in the same experimental setup. A distinct, albeit not vascular, expression of BST-2 was found in spleen and lymph nodes, consistent with its known expression in plasmacytoid dendritic cells.[23] Interestingly, expression of

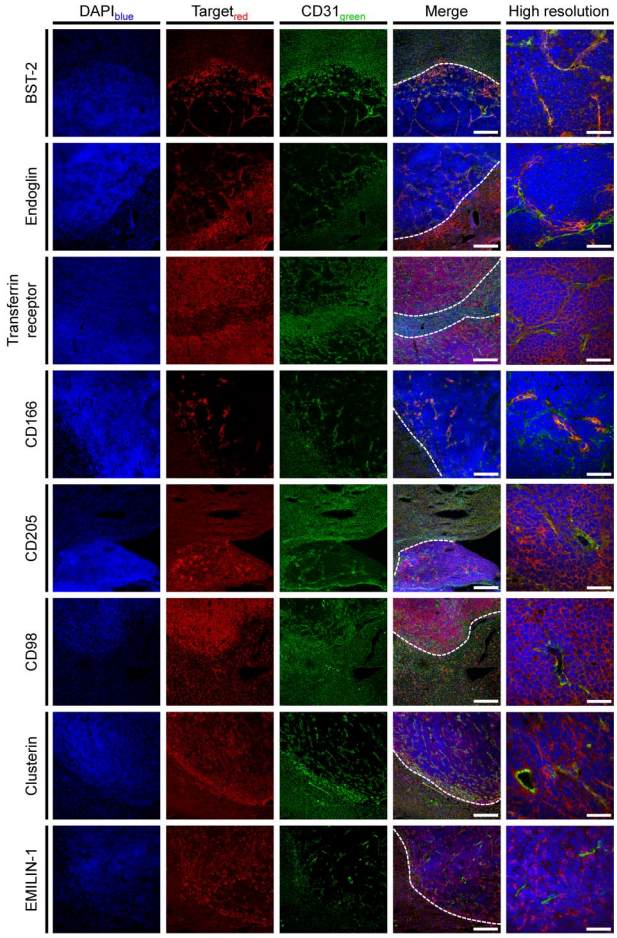

Figure 3. Validation of DeepQuanTR results. Immunostainings of the lymphoma/normal liver border (scale bars represent 200 μm) and with higher magnification of hepatic lymphoma lesions (scale bars represent 50 μm) using antibodies against 8 candidate antigens found to be up-regulated in the proteomic analyses are presented. Proteins of interest are shown in red, CD31 in green, and nuclei in blue. Lymphoma nodules are easily identified by a higher cellular density. Costaining with CD31 revealed that proteins from different localizations within the bloodstream-accessible tissue compartments (vascular endothelial cells, subendothelial matrix and stroma, perivascular tumor cells) have been modified by in vivo biotinylation and identified using DeepQuanTR. Dotted lines in merged images indicate the tumor/liver border. Slides were viewed with an LSM510 Meta confocal microscope (Carl Zeiss) using 10×/0.45 W and 40×/1.2 W water objectives and Fluorescent Mounting Medium (Dako). Images were acquired with the LSM510 Meta confocal laser scanning microscope and software provided by the manufacturer (Carl Zeiss). Images were manipulated using ImageJ software, Version 1.42q (available at http://rsb.info.nih.gov/ij/).

BST-2 could also be observed in the vasculature of subcutaneously implanted human lymphoma xenografts grown in immunodeficient mice, including Ramos, DoHH-2, and SU-DHL-4 (representing Burkitt, follicular, and diffuse large B-cell lymphomas, respectively), indicating that the expression of BST-2 in the vascular bed is apparently induced by the lymphoma environment (Figure 4A). The spatial distribution of BST-2 and CD31 expression within the lymphoma vasculature was further analyzed by confocal laser scanning microscopy, revealing a virtually complete superimposition of BST-2 and CD31 signals (Figure 4B). The pattern of BST-2 expression was recapitulated using a second monoclonal antibody specific to a different BST-2 epitope (clone 927; supplemental Figure 3).

Monoclonal anti–BST-2 antibodies home to lymphoma-associated neovasculature in vivo

Next, we investigated whether BST-2 overexpressed in angiogenic endothelium of lymphoma blood vessels could be targeted in vivo by intravenously administered antibodies. Six hours after injection of rat anti–mouse BST-2 antibodies into mice bearing disseminated A20 disease or subcutaneous A20 tumors, tumors were excised and analyzed for the presence of rat immunoglobulins, as indicated by green fluorescent staining in Figure 5A. Counterstaining with rabbit anti–mouse CD31 IgG (red) illustrated the colocalization of in vivo administered anti–BST-2 and ex vivo applied anti-CD31 antibodies in the majority of all lymphoma blood vessels (yellow color in merged images), both in hepatic lymphoma lesions and in subcutaneous tumors. Occasionally, single vessels or branches appeared to be BST-2$^-$ (hollow arrowhead, Figure 5A), a finding that is probably the result of a transient blood vessel occlusion in vivo, as virtually all CD31$^+$ vessels were found to be BST-2$^+$ in ex vivo staining procedures. A control IgG of irrelevant specificity did not accumulate in lymphoma tissues under identical conditions (Figure 5A), indicating that the observed homing to lymphoma-associated blood vessels was specific and antigen-dependent. Similarly, a second anti–BST-2 antibody exhibited an identical targeting performance (supplemental Figure 4)

Targeting BST-2 inhibits lymphoma growth

Having demonstrated that BST-2 can be successfully targeted in vivo, we performed therapy experiments in mice bearing subcutaneous lymphoma tumors, featuring 3 once-weekly intravenous administrations (5 mg/kg) of the 2 independent monoclonal antibodies directed against distinct BST-2 epitopes (clones 129c and 927). Both antibodies were significantly more potent in inhibiting lymphoma growth than equal amounts of nontargeting IgG and inhibited tumor growth by 44% (clone 129c; $P = .014$) and 48% (clone 927; $P = .008$), respectively (Figure 5B). Normal animal behavior and the absence of weight loss indicated that anti–BST-2 therapy was well tolerated (Figure 5C).

BST-2 is expressed in human lymphoma vasculature

Finally, we validated the expression of the human homolog of mouse BST-2 in specimens of human lymphoma by immunohistochemistry. In analogy to mouse lymphoma, BST-2 was detectable in the vasculature of multiple aggressive and indolent non-Hodgkin lymphoma subtypes, including diffuse large B-cell lymphoma, Burkitt lymphoma, mantle cell lymphoma, follicular lymphoma, and chronic lymphocytic leukemia (Figure 6A-E). In certain cases, tumor cells also were found to strongly express BST-2 in addition to vasculature, as illustrated in a Burkitt lymphoma specimen (Figure 6B). Again, BST-2 colocalized with the endothelial marker von Willebrand factor (Figure 6G-I).

Discussion

Using terminal perfusion of lymphoma-bearing mice and chemical proteomics procedures, we have established and characterized an atlas of proteins expressed in close association with the neovasculature of nodal and extranodal lymphoma lesion while being virtually undetectable in normal organs. Previously, the identification of markers of angiogenesis has mainly relied either by transcriptomic studies[24] or by proteomic profiling of physically separated endothelial plasma membranes.[25] In our study, from a total of 271 proteins that were simultaneously identified at all 3 lymphoma localizations, 58 showed an average DeepQuanTR protein expression value more than 2.30 (corresponding to a $>$ 10-fold up-regulation compared with the normal organ), representing promising candidates for a detailed expression analysis. Some of these proteins have previously been described as

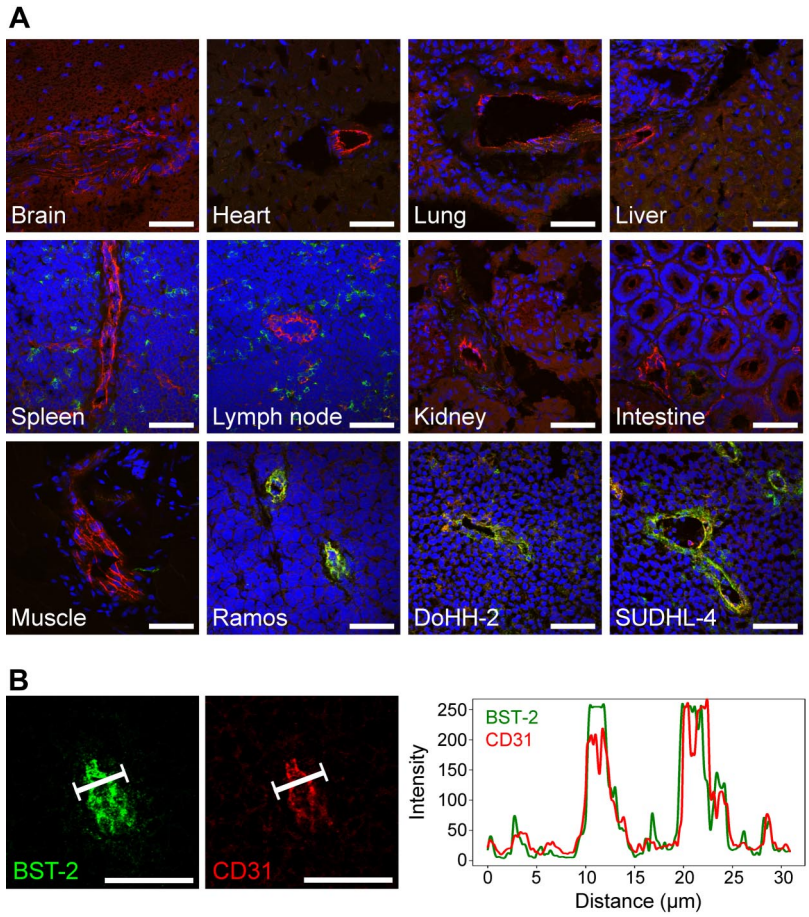

Figure 4. Expression of BST-2 in normal mouse organs and lymphoma xenografts. (A) Three-color confocal images of BST-2 staining (clone 129c, green), CD31 staining (red), and 4,6-diamidino-2-phenylindole counterstaining (blue) are shown. Although being undetectable in the vasculature of brain, heart, lung, liver, spleen, lymph nodes, kidney, intestine, and skeletal muscle, BST-2 was readily detectable in different lymphoma xenografts (Ramos, DoHH-2, SUDHL-4) in the same experiment, colocalizing to CD31 (yellow). As expected, a scattered cellular, but not vascular, expression of BST-2 was observed in lymphoid tissues. (B) Graphs displaying the spatial distribution of BST-2 and CD31 fluorescent signals in confocal microscopy were virtually superimposable. Scale bars represent 50 μm. Slides were viewed with an LSM510 Meta confocal microscope (Carl Zeiss) using 10×/0.45 W and 40×/1.2 W water objectives and Fluorescent Mounting Medium (Dako). Images were acquired with the LSM510 Meta confocal laser scanning microscope and software provided by the manufacturer (Carl Zeiss). Images were manipulated using ImageJ software, Version 1.42q (available at http://rsb.info.nih.gov/ij/).

either tumor up-regulated and/or expressed in tumor-associated neovasculature (supplemental Table 2). In accordance with previous observations, several serum components were found among the most differentially expressed proteins in neoplastic lesions (eg, complement C1q, coagulation factor V, complement factor B).[18] So far, it is not clear whether this observation results from the biotinylation of provisional tumor stroma that is known to contain blood coagulation products[26] or from the biotinylation of thrombotic events in tumor vasculature. Because of their abundance in blood, serum components were not further considered as candidate antigens for pharmacodelivery applications. In the future, the use of certain reactive derivatives of biotin with impaired extravasation properties (eg, charge, size) could potentially restrict the proteomic investigation to endothelial markers of lymphoma blood vessels.

The most interesting novel vascular marker of lymphoma identified in this study was BST-2 (also termed CD317, tetherin, or HM1.24). BST-2 was originally identified as a type II membrane glycoprotein with an unusual topology (one-pass transmembrane domain and C-terminal glycosylphosphatidylinositol anchor) that is preferentially overexpressed on multiple myeloma cells.[27,28] More recently, BST-2 has also been proposed as a tumor-associated antigen expressed in some solid tumor cell lines.[29-31] Furthermore, BST-2 has been found to block the release of enveloped particles (eg, HIV-1, Marburg virus, and Ebola virus) and may therefore be an important component of the antiviral innate immune defense.[32,33] This working hypothesis is supported by recent findings that HIV-1 viral protein U (Vpu) neutralizes the type I interferon up-regulated BST-2 expression by binding and thereby directing its β-TrCP2–dependent degradation.[34]

To our knowledge, expression of BST-2 in tumor vascular endothelium has not been described before. We did observe a scattered, albeit not vascular expression of BST-2 in normal lymphoid tissues, consistent with its known expression on mouse plasmacytoid dendritic cells.[23] Nevertheless, BST-2 was found to be up-regulated in lymphoma lesions developing in lymphoid organs in our proteomic analyses, possibly reflecting differences in accessibility of vascular endothelium and plasmacytoid dendritic cells and/or in absolute antigen abundance. Furthermore, BST-2 was detectable in blood vessels of indolent and aggressive non-Hodgkin lymphomas. In some cases, BST-2 was also strongly expressed by the lymphoma cells themselves, which can even be considered as an advantage for targeted pharmacodelivery strategies. Considering its restricted expression pattern targeting BST-2 with monoclonal antibodies or antibody derivatives might exert minimal unintended side effects. Indeed, therapy with 2 nonrelated monoclonal antibodies targeting distinct BST-2 epitopes significantly delayed lymphoma growth without apparent toxicities in mice. In principle, this antibody-induced tumor-growth delay could be explained either by antibody-dependent cell-mediated cytotoxicity (ADCC), complement-dependent cytotoxicity, or functional blocking (or a combination thereof). Indeed, antibodies of the rat IgG2b isotype have shown to be effective in promoting ADCC[35] and to eliminate disseminated human lymphoma in Scid mice.[36] However, the treatment of mice inoculated subcutaneously with human non-Hodgkin lymphoma B cells resulted in a minor tumor-growth reduction, even though murine macrophages were present in areas in these tumors that were depleted of tumor cells.[36] In humans, an ADCC-mediating monoclonal antibody to BST-2 has been reported to be well tolerated in phase 1 and 2 clinical trials in patients with multiple myeloma.[31]

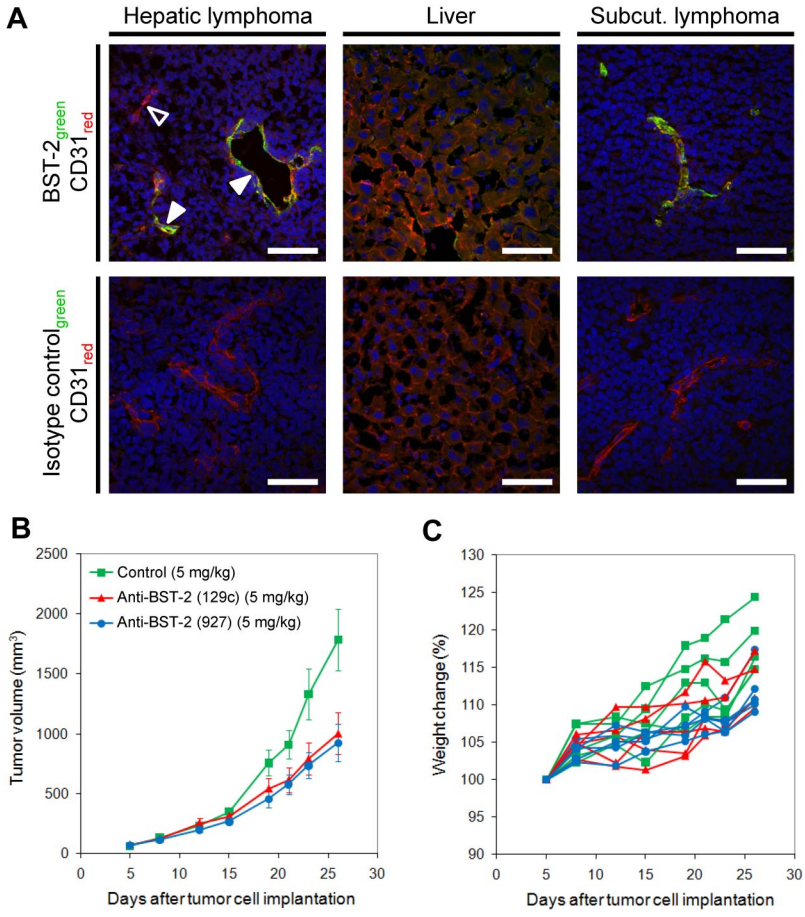

Figure 5. Monoclonal antibodies specific to BST-2 accumulate on lymphoma blood vessels and inhibit lymphoma growth in vivo. (A) A monoclonal rat anti–BST-2 antibody (clone 927) was intravenously injected into BALB/c mice bearing systemic or subcutaneous A20 lymphomas. Tumors and normal liver were excised 6 hours after injection, sectioned, and examined for the presence of rat IgG using donkey anti–rat Alexa Fluor 488 (green). Endothelial cells (CD31) were outlined in red. Although the anti–BST-2 antibody efficiently homed to lymphoma neovasculature in vivo (solid arrowheads), an isotype-matched control IgG did not accumulate on lymphoma blood vessels under identical experimental conditions. The hollow arrowhead indicates a BST-2–negative vessel that was most probably not perfused in vivo. Scale bars represent 50 μm. Slides were viewed with an LSM510 Meta confocal microscope (Carl Zeiss) using 10×/0.45 W and 40×/1.2 W water objectives and Fluorescent Mounting Medium (Dako). Images were acquired with the LSM510 Meta confocal laser scanning microscope and software provided by the manufacturer (Carl Zeiss). Images were manipulated using ImageJ software, Version 1.42q (available at http://rsb.info.nih.gov/ij/). (B) Tumor growth curves of A20 lymphomas subcutaneously implanted into BALB/c mice, treated with anti–BST-2 antibody 129c (5 mg/kg, 5 mice), anti–BST-2 antibody 927 (5 mg/kg, 5 mice), or isotype-matched control antibody (5 mg/kg, 4 mice). Treatment was administered intravenous once weekly for a period of 3 weeks. Both BST-2 antibodies significantly inhibited lymphoma growth ($P = .014$ and $P = .008$, respectively). (C) The lack of weight loss in each animal indicates that anti–BST-2 therapy was well tolerated.

The experience of our group with human monoclonal antibody derivatives, specific to alternatively spliced extracellular matrix components such as extra-domains of fibronectin and tenascin-C,[13,14,37-39] indicates that the neovasculature in solid tumors and in hematologic malignancies is quantitatively and qualitatively different, at the molecular level, from quiescent blood vessels in normal tissues. These properties can be exploited for the antibody-based delivery of therapeutic agents to the tumor neovasculature.[9-14] Indeed, immunocytokines and

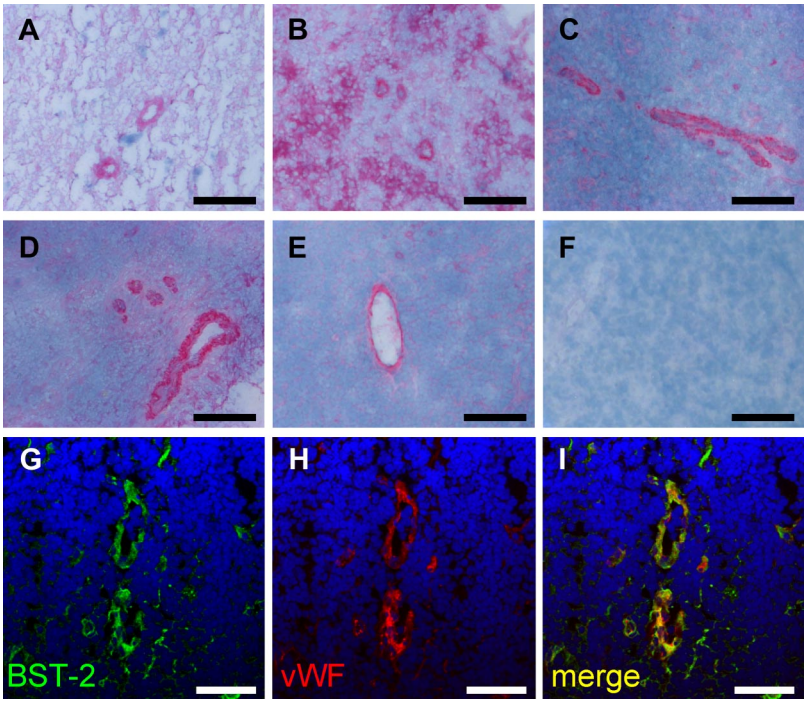

Figure 6. Expression of BST-2 in human non-Hodgkin lymphoma. BST-2 was detected in vascular structures of aggressive (A-C) and indolent (D-E) human non-Hodgkin lymphoma specimens using alkaline phosphatase–antialkaline phosphatase immunohistochemistry. Representative images of diffuse large B-cell lymphoma (A), Burkitt lymphoma (B), mantle cell lymphoma (C), follicular lymphoma (D), and chronic lymphocytic leukemia (E) are presented. Negative controls omitting the primary antibody were consistently negative (F). Although in most cases a predominant vascular staining was observed, also tumor cells were strongly immunostained in a case of Burkitt lymphoma (B). Slides were viewed with an Axiovert S100TV microscope (Carl Zeiss) using a 20×/0.40 Korr Ph2 objective and Glycergel Mounting Medium (Dako). Images were acquired using an AxioCam color camera and AxioVision software Version 4.7.1.0 (Carl Zeiss). Images were manipulated using ImageJ, Version 1.42q (available at http://rsb.info.nih.gov/ij/; A-F). Confocal images illustrate the colocalization of BST-2 and von Willebrand factor (vWF), exemplified on a section of chronic lymphocytic leukemia (G-I). Scale bars represent 100 μm (A-F) and 50 μm (G-I). Slides were viewed with an LSM510 Meta confocal microscope (Carl Zeiss) using 10×/0.45 W and 40×/1.2 W water objectives and Fluorescent Mounting Medium (Dako). Images were acquired with the LSM510 Meta confocal laser scanning microscope and software provided by the manufacturer (Carl Zeiss). Images were manipulated using ImageJ software, Version 1.42q (available at http://rsb.info.nih.gov/ij/; G-I).

radiolabeled antibodies specific to the EDA and EDB domain of fibronectin, and to the extra-domains A1 and D of tenascin-C are currently being investigated in clinical trials.[14,40] Similar pharmacodelivery strategies could be considered for derivatives of anti–BST-2 antibodies. In addition, the use of intact IgG products for the inhibition of lymphoma growth could be potentiated by suitable modifications of the immunoglobulin molecule, such as glycoengineering[41,42] or mutagenesis of the Fc antibody fragment.[43] In lymphoma, antibody-based pharmacodelivery strategies hold the promise to efficiently deliver therapeutic molecules to bulky tumor masses. It is tempting to speculate that bioactive agents (such as drugs with cleavable linkers or radionuclides) targeted to the bone marrow vascular compartment may exhibit therapeutic activity also in leukemia, given the fact that leukemic cells reside in close proximity to specialized vascular structures.[44]

The findings presented in this article could have considerable clinical relevance, considering that BST-2 is strongly expressed not only in the neovasculature of A20 lymphoma in mice, but also in blood vessels of human diffuse large B-cell lymphoma, Burkitt lymphoma, mantle cell lymphoma, follicular lymphoma, and chronic lymphocytic leukemia.

Acknowledgments

The authors thank the Functional Genomics Center Zurich for access to the HPLC and for technical support.

This work was supported by the Swiss National Science Foundation, the ETH Zürich, the European Union (ADAMANT and IMMUNO-PDT projects), the Swiss Cancer League, the SwissBridge Foundation, and the Stammbach Foundation. C.S. receives a bursary from the Deutsche Krebshilfe.

Authorship

Contribution: C.S. and C.R. designed the project, performed experiments, analyzed results, and wrote the manuscript; H.K. performed the proteomic analysis; B.B. performed perfusion experiments; T.F. designed the DeepQuanTR software and analyzed data; W.K. provided human lymphoma specimens; and D.N. designed the project, analyzed data, and wrote and reviewed the manuscript.

Conflict-of-interest disclosure: The authors declare no competing financial interests.

Correspondence: Dario Neri, Institute of Pharmaceutical Sciences, Department of Chemistry and Applied Biosciences, ETH Zurich, Wolfgang-Pauli-Strasse 10, CH-8093 Zurich, Switzerland; e-mail: neri@pharma.ethz.ch; or Christoph Roesli, Institute of Pharmaceutical Sciences, Department of Chemistry and Applied Biosciences, ETH Zurich, Wolfgang-Pauli-Strasse 10, CH-8093 Zurich, Switzerland; e-mail: christoph.roesli@pharma.ethz.ch.

References

1. Neri D, Bicknell R. Tumour vascular targeting. *Nat Rev Cancer.* 2005;5(6):436-446.
2. Schrama D, Reisfeld RA, Becker JC. Antibody targeted drugs as cancer therapeutics. *Nat Rev Drug Discov.* 2006;5(2):147-159.
3. Schliemann C, Neri D. Antibody-based targeting of the tumor vasculature. *Biochim Biophys Acta.* 2007;1776(2):175-192.
4. Carter PJ. Potent antibody therapeutics by design. *Nat Rev Immunol.* 2006;6(5):343-357.
5. Adams GP, Weiner LM. Monoclonal antibody therapy of cancer. *Nat Biotechnol.* 2005;23(9):1147-1157.
6. Thorpe PE. Vascular targeting agents as cancer therapeutics. *Clin Cancer Res.* 2004;10(2):415-427.
7. Dennis MS, Jin H, Dugger D, et al. Imaging tumors with an albumin-binding Fab, a novel tumor-targeting agent. *Cancer Res.* 2007;67(1):254-261.
8. Singh Jaggi J, Henke E, Seshan SV, et al. Selective alpha-particle mediated depletion of tumor vasculature with vascular normalization. *PLoS ONE.* 2007;2(3):e267.
9. Carnemolla B, Borsi L, Balza E, et al. Enhancement of the antitumor properties of interleukin-2 by its targeted delivery to the tumor blood vessel extracellular matrix. *Blood.* 2002;99(5):1659-1665.
10. Halin C, Rondini S, Nilsson F, et al. Enhancement of the antitumor activity of interleukin-12 by targeted delivery to neovasculature. *Nat Biotechnol.* 2002;20(3):264-269.
11. Borsi L, Balza E, Carnemolla B, et al. Selective targeted delivery of TNFα to tumor blood vessels. *Blood.* 2003;102(13):4384-4392.
12. Marlind J, Kaspar M, Trachsel E, et al. Antibody-mediated delivery of interleukin-2 to the stroma of breast cancer strongly enhances the potency of chemotherapy. *Clin Cancer Res.* 2008;14(20):6515-6524.
13. Schliemann C, Palumbo A, Zuberbuhler K, et al. Complete eradication of human B-cell lymphoma xenografts using rituximab in combination with the immunocytokine L19-IL2. *Blood.* 2009;113(10):2275-2283.
14. Sauer S, Erba PA, Petrini M, et al. Expression of the oncofetal ED-B-containing fibronectin isoform in hematologic tumors enables ED-B-targeted 131I-L19SIP radioimmunotherapy in Hodgkin lymphoma patients. *Blood.* 2009;113(10):2265-2274.
15. Cheson BD, Leonard JP. Monoclonal antibody therapy for B-cell non-Hodgkin's lymphoma. *N Engl J Med.* 2008;359(6):613-626.
16. Senter PD. Potent antibody drug conjugates for cancer therapy. *Curr Opin Chem Biol.* 2009;13(3):235-244.
17. Rizzieri DA, Akabani G, Zalutsky MR, et al. Phase 1 trial study of 131I-labeled chimeric 81C6 monoclonal antibody for the treatment of patients with non-Hodgkin lymphoma. *Blood.* 2004;104(3):642-648.
18. Rybak JN, Ettorre A, Kaissling B, Giavazzi R, Neri D, Elia G. In vivo protein biotinylation for identification of organ-specific antigens accessible from the vasculature. *Nat Methods.* 2005;2(4):291-298.
19. Roesli C, Neri D, Rybak JN. In vivo protein biotinylation and sample preparation for the proteomic identification of organ- and disease-specific antigens accessible from the vasculature. *Nat Protoc.* 2006;1(1):192-199.
20. Castronovo V, Waltregny D, Kischel P, et al. A chemical proteomics approach for the identification of accessible antigens expressed in human kidney cancer. *Mol Cell Proteomics.* 2006;5(11):2083-2091.
21. Scheurer SB, Rybak JN, Roesli C, et al. Identification and relative quantification of membrane proteins by surface biotinylation and two-dimensional peptide mapping. *Proteomics.* 2005;5(11):2718-2728.
22. Passineau MJ, Siegal GP, Everts M, et al. The natural history of a novel, systemic, disseminated model of syngeneic mouse B-cell lymphoma. *Leuk Lymphoma.* 2005;46(11):1627-1638.
23. Blasius AL, Giurisato E, Cella M, Schreiber RD, Shaw AS, Colonna M. Bone marrow stromal cell antigen 2 is a specific marker of type I IFN-producing cells in the naive mouse, but a promiscuous cell surface antigen following IFN stimulation. *J Immunol.* 2006;177(5):3260-3265.
24. St Croix B, Rago C, Velculescu V, et al. Genes expressed in human tumor endothelium. *Science.* 2000;289(5482):1197-1202.
25. Oh P, Li Y, Yu J, et al. Subtractive proteomic mapping of the endothelial surface in lung and solid tumours for tissue-specific therapy. *Nature.* 2004;429(6992):629-635.
26. Dvorak HF. Tumors: wounds that do not heal. Similarities between tumor stroma generation and wound healing. *N Engl J Med.* 1986;315(26):1650-1659.
27. Goto T, Kennel SJ, Abe M, et al. A novel membrane antigen selectively expressed on terminally differentiated human B cells. *Blood.* 1994;84(6):1922-1930.
28. Ohtomo T, Sugamata Y, Ozaki Y, et al. Molecular cloning and characterization of a surface antigen preferentially overexpressed on multiple myeloma cells. *Biochem Biophys Res Commun.* 1999;258(3):583-591.
29. Walter-Yohrling J, Cao X, Callahan M, et al. Identification of genes expressed in malignant cells that promote invasion. *Cancer Res.* 2003;63(24):8939-8947.
30. Wang W, Nishioka Y, Ozaki S, et al. HM1.24 (CD317) is a novel target against lung cancer for immunotherapy using anti-HM1.24 antibody. *Cancer Immunol Immunother.* 2009;58(6):967-976.
31. Kawai S, Azuma Y, Fujii E, et al. Interferon-alpha enhances CD317 expression and the antitumor activity of anti-CD317 monoclonal antibody in renal cell carcinoma xenograft models. *Cancer Sci.* 2008;99(12):2461-2466.
32. Jouvenet N, Neil SJ, Zhadina M, et al. Broad-spectrum inhibition of retroviral and filoviral particle release by tetherin. *J Virol.* 2009;83(4):1837-1844.

33. Neil SJ, Zang T, Bieniasz PD. Tetherin inhibits retrovirus release and is antagonized by HIV-1 Vpu. *Nature.* 2008;451(7177):425-430.

34. Mangeat B, Gers-Huber G, Lehmann M, Zufferey M, Luban J, Piguet V. HIV-1 Vpu neutralizes the antiviral factor Tetherin/BST-2 by binding it and directing its beta-TrCP2-dependent degradation. *PLoS Pathog.* 2009;5(9):e1000574.

35. Hale G, Clark M, Waldmann H. Therapeutic potential of rat monoclonal antibodies: isotype specificity of antibody-dependent cell-mediated cytotoxicity with human lymphocytes. *J Immunol.* 1985;134(5):3056-3061.

36. de Kroon JF, de Paus RA, Kluin-Nelemans HC, et al. Anti-CD45 and anti-CD52 (Campath) monoclonal antibodies effectively eliminate systematically disseminated human non-Hodgkin's lymphoma B cells in Scid mice. *Exp Hematol.* 1996; 24(8):919-926.

37. Kaspar M, Zardi L, Neri D. Fibronectin as target for tumor therapy. *Int J Cancer.* 2006;118(6): 1331-1339.

38. Brack SS, Silacci M, Birchler M, Neri D. Tumor-targeting properties of novel antibodies specific to the large isoform of tenascin-C. *Clin Cancer Res.* 2006;12(10):3200-3208.

39. Pedretti M, Soltermann A, Arni S, Weder W, Neri D, Hillinger S. Comparative immunohistochemistry of L19 and F16 in non-small cell lung cancer and mesothelioma: two human antibodies investigated in clinical trials in patients with cancer. *Lung Cancer.* 2009;64(1):28-33.

40. Santimaria M, Moscatelli G, Viale GL, et al. Immunoscintigraphic detection of the ED-B domain of fibronectin, a marker of angiogenesis, in patients with cancer. *Clin Cancer Res.* 2003;9(2): 571-579.

41. Ferrara C, Stuart F, Sondermann P, Brunker P, Umana P. The carbohydrate at FcgammaRIIIa Asn-162: an element required for high affinity binding to non-fucosylated IgG glycoforms. *J Biol Chem.* 2006;281(8):5032-5036.

42. Nimmerjahn F, Ravetch JV. Divergent immunoglobulin g subclass activity through selective Fc receptor binding. *Science.* 2005;310(5753):1510-1512.

43. Lazar GA, Dang W, Karki S, et al. Engineered antibody Fc variants with enhanced effector function. *Proc Natl Acad Sci U S A.* 2006;103(11): 4005-4010.

44. Sipkins DA, Wei X, Wu JW, et al. In vivo imaging of specialized bone marrow endothelial microdomains for tumour engraftment. *Nature.* 2005; 435(7044):969-973.